Available online at www.easd.procedia.org
EASD Procedia EURODYN (2026) 2460-2474

EASD Procedia

EURODYN 2026
XIII International Conference on Structural Dynamics
M. Beer, C. Papadimitriou, H. Jensen, J. Chen, M. Broggi, J. Behrensdorf (eds.)
Hannover, Germany, 27.09.–01.10 2026

NUMERICAL INVESTIGATION OF AUXETIC SANDWICH PLATES UNDER BLAST LOADING

Rahul Reddy Gajjala, George Joy and Prasun Jana

Indian Institute of Technology Kharagpur
West Bengal, India
e-mail: gajjalarahulreddy@gmail.com

Keywords: Sandwich structure, Re-entrant auxetic core, Conventional Weapons Effects Program (CONWEP), ABAQUS, Johnson–Cook material model, Johnson–Cook damage model.

Abstract. *Auxetic sandwich structures are emerging as promising candidates for blast mitigation due to their lateral contraction response under compression, which enhances load redistribution and energy dissipation. This study numerically investigates the blast response of a sandwich plate with a re-entrant auxetic core to understand its deformation and energy absorption mechanisms under severe impulsive loading. The finite element simulations are carried out in ABAQUS using the Dynamic Explicit solver. The metallic face sheets and the auxetic core are modelled with S4R shell elements with hourglass control, and strain rate-dependent material behaviour is incorporated through the Johnson–Cook constitutive parameters along with its damage criteria. The blast load is applied using the Conventional Weapons Effects Program (CONWEP) approach to simulate an air-borne explosive with different shock factors. The computational model is initially validated against the results reported in the literature. A parametric study is then performed by varying the geometric parameters of the re-entrant unit cell as well as the shock factor of the blast load. The structural response is examined in terms of specific energy absorption (SEA), plastic dissipation, and the maximum displacement of the front and back face sheets. The findings from this research aim to provide insight into the role of auxetic geometry on blast resistance characteristics of lightweight sandwich structures.*

ISSN:2311-9020 © 2026 The Authors. Published by EASD Procedia.
Peer-review under responsibility of the Organizing Committee of EURODYN 2026.
doi: 10.47964/1326.10842.529

1 INTRODUCTION

Auxetic materials [1, 2] exhibit a negative Poisson's ratio (NPR), meaning that they expand laterally when subjected to tensile loading and contract laterally under compression. Because of this deformation mechanism, the volumetric strain increases, which improves the energy absorption capability [3, 4] compared with conventional materials. Owing to this behavior, auxetic structures show better load transfer within the structure. As a result, they have been considered for several engineering applications such as blast and impact protection [5–8], vibration attenuation [9, 10], and improved resistance to indentation [11, 12]. Therefore, auxetic geometries are increasingly being investigated for lightweight structures subjected to severe dynamic loading.

Auxetic structures are often used as cores in sandwich configurations, where the core layer plays an important role in absorbing and dissipating energy generated during blast loading. Because of their high stiffness-to-weight ratio, sandwich structures [13] with auxetic cores are commonly considered for lightweight protective structures subjected to severe dynamic loads such as blasts.

To understand the effectiveness of such configurations under blast loading, several studies have investigated the response of sandwich structures with different core designs. In this context, a numerical investigation by Derseth et al. [14] examined hybrid metallic sandwich structures subjected to air blast loading. Based on their finite element simulations, it was observed that the hybrid configuration combining square honeycomb cores with X-shaped corrugated sheets exhibited better blast shielding capability, with lower damage, higher energy dissipation, and smaller back-sheet displacement. An experimental and numerical study by Novak et al. [15] investigated the blast response of sandwich composite panels with chiral auxetic cores, with a detailed parametric analysis of core geometry. Their results show that increasing cover plate thickness reduces maximum displacement while thinner plates improve SEA, and that cell length has a more significant influence than amplitude, with the auxetic core achieving about 10% lower displacement and higher energy absorption compared to a monolithic plate of the same mass. The work by Chen et al. [16] examines the blast response of sandwich panels incorporating 3D-printed gradient auxetic chiral cores under varying gradient configurations and impulse levels. Their findings indicate that negative gradient designs result in the lowest permanent deflection and improved resistance, while increasing impulse leads to greater plastic deformation in the face sheets along with shear and tensile tearing in the core. Similar works addressing the air-blast behaviour on sandwich structures with auxetic cores can be found in Ref. [17–19].

The re-entrant geometry is one of the most widely studied auxetic configurations. Consequently, it has been extensively investigated through theoretical, experimental, and numerical approaches in the literature. For example, the numerical study by Imbalzano et al. [20] investigates the blast response of sandwich panels with honeycomb and re-entrant auxetic cores using finite element simulations, showing that the re-entrant geometry draws material into the loaded region and significantly reduces back-face deformation while improving energy absorption. Their conclusions further indicate that variations in re-entrant cell angle and relative density strongly influence the deformation mode and blast mitigation capability, with higher auxeticity leading to improved performance. A numerical study by Rai et al. [21] investigates the blast response of sandwich panels with re-entrant auxetic cores, focusing on the influence of cell angle, wall thickness, core height, charge mass, and stand-off distance on structural response. The results show that these geometric parameters significantly affect peak deflection, energy absorption, and impulse transfer, with core layering further modifying the deformation behaviour under blast loading. The work by Jin et al. [22] examines the air blast response of

sandwich panels with graded re-entrant auxetic cores, considering different core arrangements such as uniform, gradient, and cross configurations. The results show that the distribution and arrangement of re-entrant cells significantly influence face-sheet deflection and energy absorption, with graded and cross configurations reducing peak deflection and improving blast mitigation performance. A numerical investigation by Walkowiak et al. [23] examines the influence of different core topologies, including re-entrant auxetic lattice cores, on the air-blast response of sandwich-structured composites under controlled geometric and mass conditions. The results show that auxetic lattice cores achieve up to about 70% reduction in transmitted peak load while increasing energy dissipation through core plasticization, and their geometry-dependent deformation reduces lower face deflection and prevents crack initiation compared to other core types. Several other studies examining the blast response of sandwich plates with re-entrant and modified re-entrant auxetic cores are reported in Ref. [24–29].

From the literature it can be noticed that many studies have examined the air blast response of sandwich plates with re-entrant auxetic cores. However, a systematic investigation of the influence of geometric parameters of the re-entrant core is still lacking. In addition, the effect of these parameters under conditions involving material damage has not been adequately addressed. As the re-entrant configuration represents the fundamental auxetic geometry, a detailed parametric assessment at various intensities of blasts incorporating damage becomes necessary. The present study addresses this gap by examining the role of core geometry on the blast response while accounting for damage effects and variation of charge weight of blast.

The manuscript is arranged into four sections in a sequential manner. In Section 2, the finite element model developed in ABAQUS is described, with details of the material behaviour and the associated damage modelling for blast-loaded sandwich plates. Section 3 presents the validation of the numerical model, where the finite element response is compared with available results to establish its accuracy. The response of the sandwich configuration with a re-entrant core under blast loading is discussed in Section 4, along with the influence of the core parameters. The article ends with the key observations and the scope for further work which are mentioned in Section 5.

2 FINITE ELEMENT SIMULATION SETUP OF BLAST LOAD ON SANDWICH PLATE

The finite element simulations on the sandwich plates exposed to air blast loads are carried out using the dynamic explicit solver available in ABAQUS. The cellular metallic core is modeled using four-node shell elements with reduced integration, together with five Simpson thickness integration points. This element type is well suited for modelling thin-walled cellular structures while ensuring numerical stability during dynamic analyses. Depending on the thickness of the face sheets, they are modeled either using shell or three-dimensional elements. When the thickness is relatively small, the face sheets are discretized using S4R shell elements, whereas for comparatively thicker configurations three-dimensional brick elements are employed. The cellular core is connected to the face sheets at the top and bottom interfaces using tie constraints in ABAQUS/Explicit so that both components deform together without relative separation at the interface.

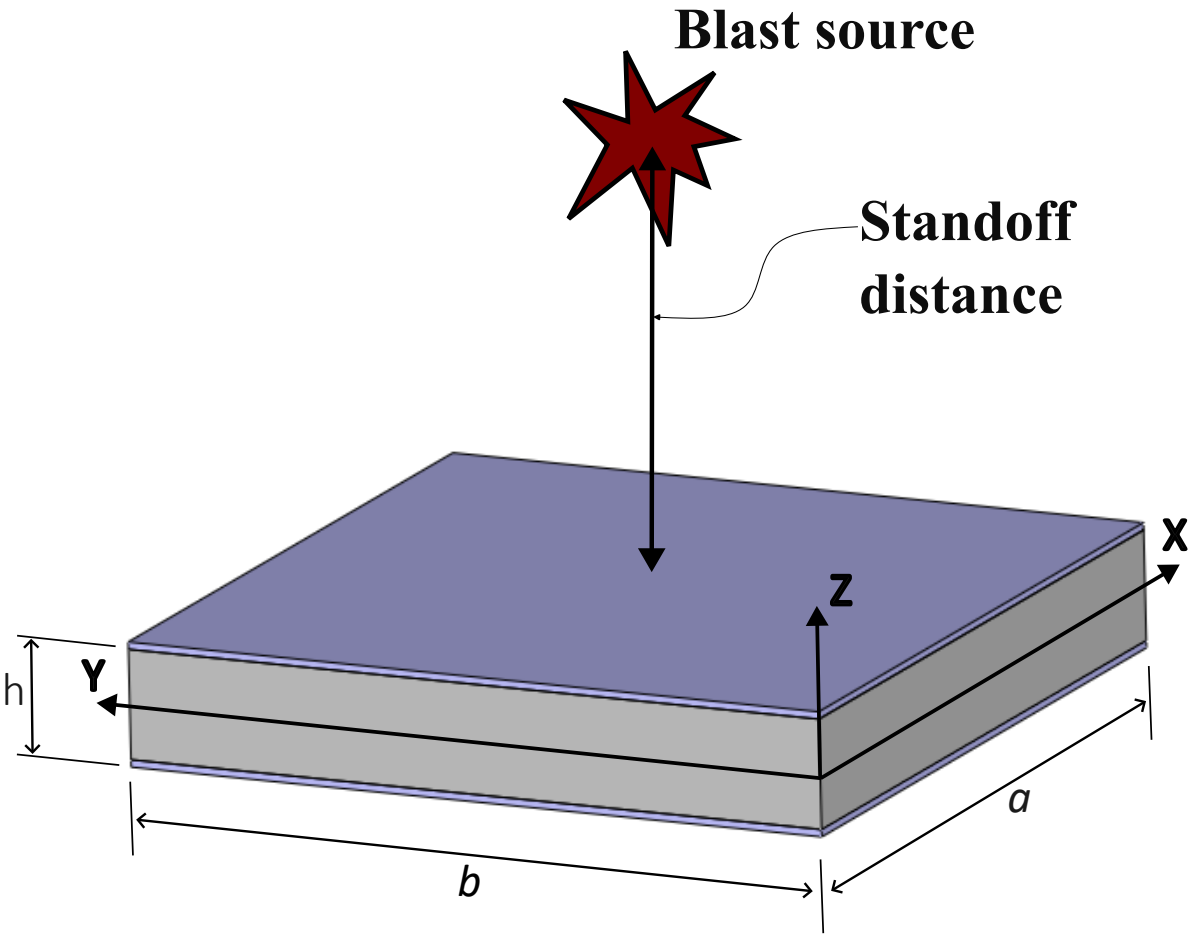


Figure 1: Schematic representation of the blast load on the sandwich plate.

The TNT charge of blast is applied at the center of plate at a distance above the top facesheet as shown in Fig. 1. The edges of the sandwich plate are subjected to clamped boundary conditions throughout the study. Due to the geometric symmetry of the configuration, only one-quarter of the model is considered in the simulations to reduce the computational cost. Appropriate symmetry boundary conditions are imposed along the two edges passing through the center of the plate. Along the edge parallel to the X-direction, the rotation about the X-axis, the displacement along the Y-direction, and the rotation about the Z-axis are constrained. Similarly, along the edge parallel to the Y-direction, the rotation about the Y-axis, the displacement along the X-direction, and the rotation about the Z-axis are constrained. These conditions ensure that the response of the quarter model represents the behaviour of the full plate.

The material behaviour of the metallic constituents is described using the Johnson-Cook (JC) constitutive model (see Ref. [30]), which accounts for the combined effects of plastic strain, strain rate, and temperature under dynamic loading conditions. The flow stress of Johnson-Cook model is expressed as

$$\sigma = [A + B\varepsilon^n]\,[1 + C\ln(\dot{\varepsilon}^*)]\,[1 - (T^*)^m] \tag{1}$$

where σ is the equivalent flow stress, ε is the equivalent plastic strain, and $\dot{\varepsilon}^*$ is the dimensionless plastic strain rate defined as $\dot{\varepsilon}/\dot{\varepsilon}_0$, with $\dot{\varepsilon}_0$ being the reference strain rate. The term T^* represents

the homologous temperature, defined as $(T-T_{\text{ref}})/(T_m-T_{\text{ref}})$, where T is the current temperature, T_{ref} is the reference temperature, and T_m is the melting temperature of the material. The material constants A, B, n, C, and m correspond to the initial yield stress, strain hardening coefficient, strain hardening factor, strain rate sensitivity coefficient, and thermal softening coefficient, respectively. The first term in eqn. 1 represents strain hardening, the second term accounts for strain rate effects, and the third term captures thermal softening. Owing to its simple form and ability to represent large strain deformation under high strain-rate conditions, the JC model is widely adopted in simulations of impact and blast problems.

The failure behaviour of the metallic components is modeled using the Johnson-Cook damage formulation as discussed in Ref. [31]. According to JC damage model, the equivalent plastic strain at onset of damage is expressed as

$$\varepsilon_f = [D_1 + D_2 \exp(D_3\sigma^*)]\,[1 + D_4 \ln(\dot{\varepsilon}^*)]\,[1 + D_5 T^*] \tag{2}$$

where D_1, D_2, D_3, D_4, and D_5 are material constants. The term $\sigma^* = \sigma_m/\bar{\sigma}$ denotes the stress triaxiality, where σ_m is the mean stress and $\bar{\sigma}$ is the von Mises equivalent stress. The term $\dot{\varepsilon}^* = \dot{\varepsilon}/\dot{\varepsilon}_0$ represents the dimensionless strain rate, and T^* is the homologous temperature defined based on the current, reference, and melting temperatures of the material. Based on ε_f, the damage initiation parameter is defined as

$$JCCRT = \sum \frac{\Delta\varepsilon}{\varepsilon_f} \tag{3}$$

where $\Delta\varepsilon$ is the increment of equivalent plastic strain. The damage initiation specifies the onset of failure, i.e., the point at which the material begins to lose its stiffness. The damage initiates when $JCCRT$ reaches unity.

Following damage initiation, the degradation of stiffness is governed by a displacement-based damage evolution law. A linear degradation model is adopted, in which the damage parameter D evolves with the effective plastic displacement and reduces the material stiffness by a factor of $(1 - D)$. The degradation is assumed to be isotropic, resulting in uniform stiffness reduction in all directions. The displacement at failure is specified to define complete material failure corresponding to $D = 1$, and in the present study this value is taken as 20% of the characteristic length of the element. When D approaches unity, the element effectively loses its load-carrying capacity and is removed during the corresponding time step in the finite element analysis. However, in the current study, the element deletion is not activated; Therefore, the value of D is limited to 0.99, for which the element almost loses its entire stiffness.

In the present simulations, the blast pressure acting on the front face of the sandwich panel is defined through the Conventional Weapons Effects Program (CONWEP) option provided in ABAQUS. This approach evaluates the pressure-time history generated by an explosive charge based on empirical blast relations and applies the resulting load directly on the structure. The simulations are performed using a dynamic explicit step with nonlinear geometric effects included, while the stable time increment is automatically controlled by ABAQUS/Explicit based on the element size and material properties.

3 FINITE ELEMENT VALIDATION OF SANDWICH PLATE EXPOSED TO BLAST LOADS

To prove the simulations' authenticity, validation against the existing literature is required. For the validation purpose, the finite element model of the sandwich panel is developed consisting

of two metallic face sheets and a square honeycomb core placed between them, as it has been considered in Derseh et al. [14]. Each face sheet has a thickness of 5 mm, while the honeycomb core has a height of 51 mm with a wall thickness of 0.76 mm and a cell spacing of 30.5 mm. The overall panel dimension considered in the experiment is 610 mm × 610 mm. In order to reduce the computational cost, the geometric symmetry of the structure is utilized and only one-quarter of the panel is modeled, resulting in a computational domain of 305 mm × 305 mm. For validation in the present section, both the face sheets and the core are modeled using steel, and the same material is retained for the re-entrant core sandwich investigated in Section 4.

The face sheets are discretized using reduced integration eight-node three-dimensional brick elements. An air-burst explosion corresponding to a 3 kg TNT charge placed at a stand-off distance of 100 mm from the center of the panel is considered. The analysis is carried out using a dynamic explicit step with a total simulation time of 1.5 ms.

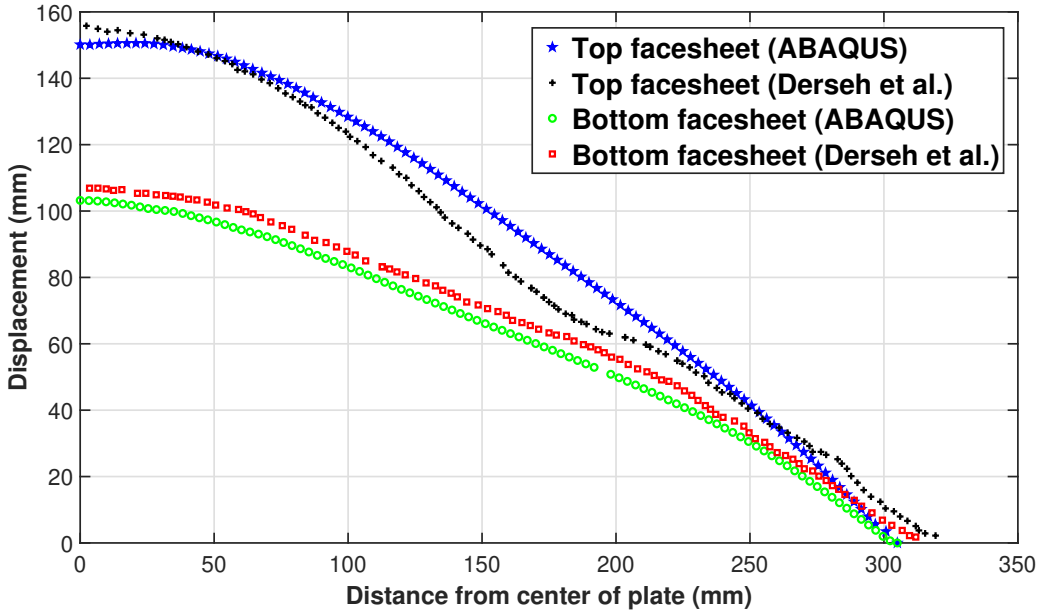


Figure 2: Finite element simulation validation of blast load with Derseh et al. [14].

The numerical results are validated with the results reported in Ref. [14], and the Johnson–Cook plasticity and damage parameters employed in the present study are also adopted from the same reference. Fig. 2 presents the comparison between the present ABAQUS simulation and the results reported in Ref. [14] in terms of displacement of the top and bottom face sheets along the edge passing through the center of the plate and extending up to the clamped boundary. It can be observed that the numerical predictions are in close agreement with the reference results for both the front and back face sheets, thereby demonstrating the accuracy of the present finite element model. The validated numerical setup is therefore employed for the subsequent simulations performed in this study.

4 RESULTS AND DISCUSSIONS

This section presents the discussions on the blast response of sandwich plate with re-entrant auxetic core. The core consists of four layers of re-entrant unit cells, and throughout this section,

the in-plane dimensions of the sandwich plate are: $a = b = 420$ mm. The sandwich height is not fixed; during parametric studies, it varies. Since the plate is clamped along all edges and the loading is symmetric, a quarter model of size 210 mm × 210 mm is considered for all the simulations. The CAD model is made in SOLIDWORKS and the one-fourth configuration of sandwich is shown in Fig. 3, where the parametric dimensions of the re-entrant unit cell are also indicated.

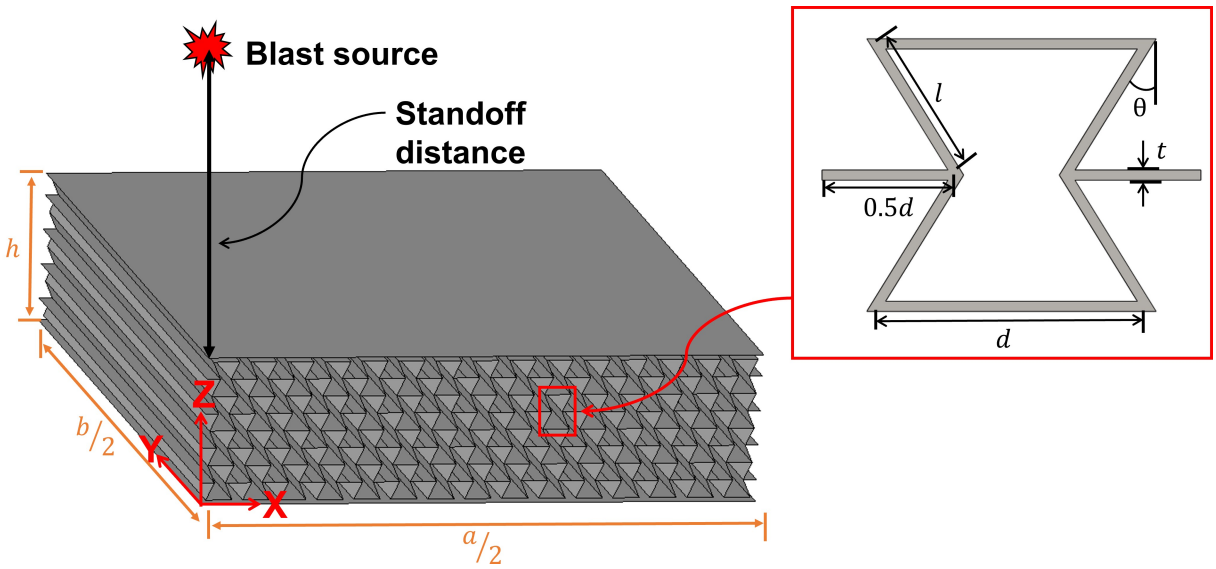


Figure 3: Schematic of the blast-loaded sandwich plate (quarter model) with a re-entrant auxetic core, showing the corresponding geometric parameters of the unit cell.

The geometry of the re-entrant auxetic unit cell is defined using four parameters, namely the inclined ligament length (l), horizontal ligament length (d), inclined ligament angle (θ), and ligament thickness (t). The baseline configuration is taken as $l = 6$ mm, $d = 10$ mm, $\theta = 30°$, and $t = 0.5$ mm. Both the face sheets and the core are made of steel, and the thickness of the top and bottom face sheets is maintained at 2 mm. All simulations are carried out using a uniform mesh size of 3 mm for both the facesheets and the re-entrant core, which was selected based on the results of the mesh convergence study for a shock factor of 4.5. The detailed results of the mesh convergence study are not presented for the sake of brevity.

The shock factor is a commonly used parameter in blast loading studies to represent the intensity of an air blast in a simplified form. It combines the effect of the explosive charge weight and the standoff distance into a single quantity, allowing different blast conditions to be compared in a consistent manner. The shock factor (SF) is taken as

$$SF = \frac{0.45}{R}\sqrt{W} \tag{4}$$

where W is the TNT charge weight and R is the standoff distance. Higher values of SF indicate a stronger blast, whereas lower values correspond to a relatively weaker blast loading. In this way, different air blast conditions can be expressed using a single parameter. In the present work, the sandwich plate is analyzed for two cases, $SF = 4.5$ and $SF = 5.5$, with a constant standoff distance (R) of 100 mm, corresponding to TNT weights of 1 kg and 1.5 kg, respectively.

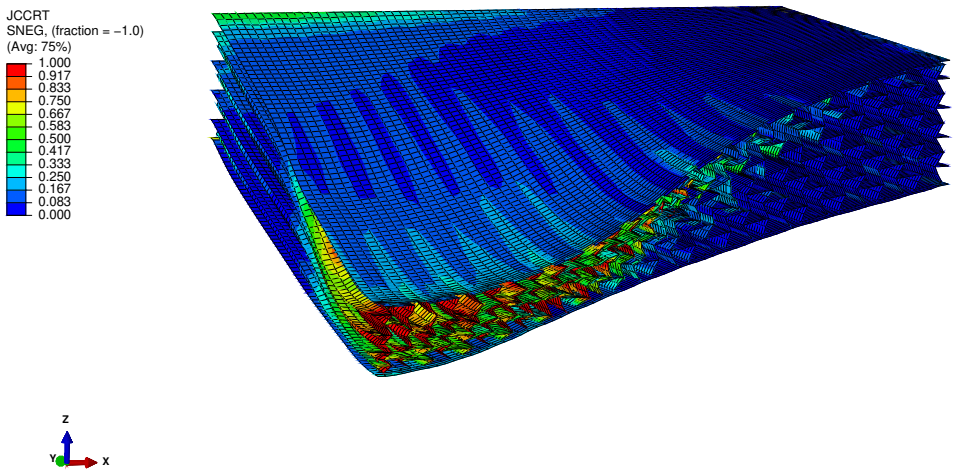


Figure 4: Deformation of the baseline sandwich plate under a blast load with a shock factor of 4.5.

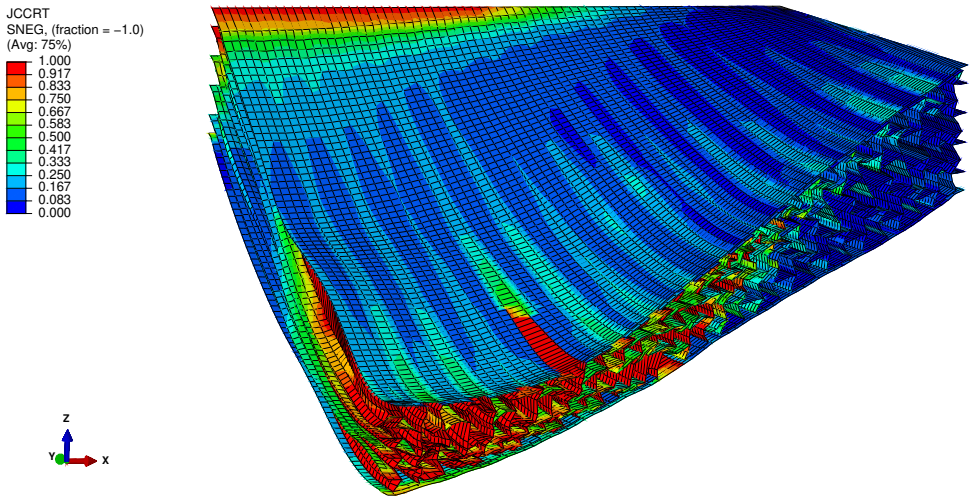
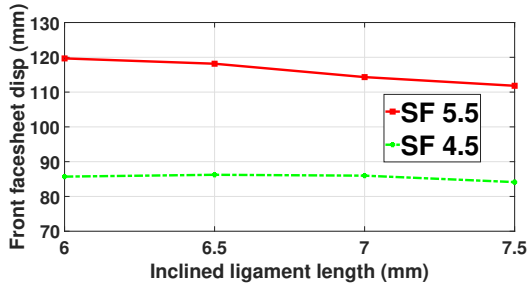


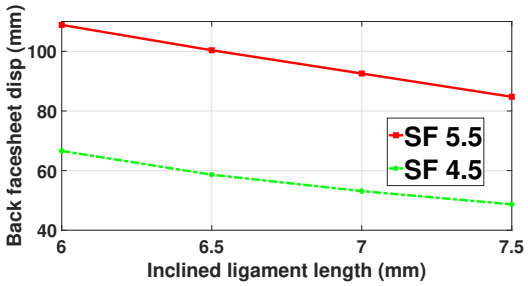
Figure 5: Deformation of the baseline sandwich plate under a blast load with a shock factor of 5.5.

The deformation of the baseline sandwich plate corresponding to $SF = 4.5$ and $SF = 5.5$ is shown in Fig. 4 and Fig. 5, respectively, at the instant where the maximum back facesheet displacement is attained. In both cases, the damage variable $JCCRT$ is also shown for all the elements, where the damaged elements ($JCCRT = 1$) are highlighted in red. It can be observed that most of the elements with $JCCRT = 1$ are concentrated in the region corresponding to the maximum deflection, indicating that the damage is primarily localized in this zone. It can be observed that the deformation of the sandwich plate is higher for the higher SF, and a larger number of elements reach $JCCRT = 1$, indicating increased damage initiation under the higher intensity of the blast loading. The clamped edge parallel to the Y-axis remains intact in both

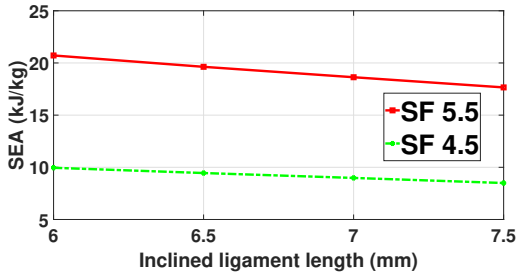
cases. However, for the higher loading case, i.e., $SF = 5.5$ (Fig. 5), damage initiaiton is observed near the clamped edge parallel to the X-axis. Such behaviour is not observed in the $SF = 4.5$ case (Fig. 4), indicating a comparatively less severe structural response.



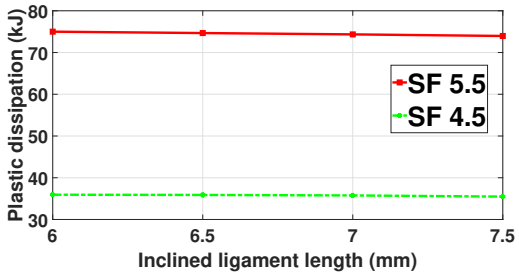
(a) Front facesheet displacement



(b) Back facesheet displacement



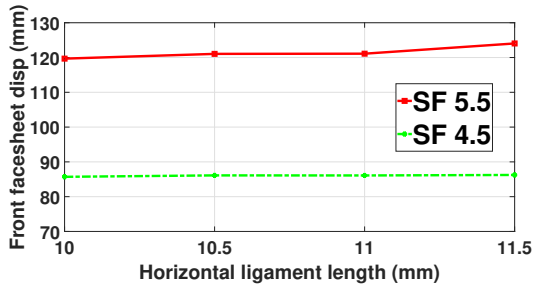
(c) Specific energy absorption



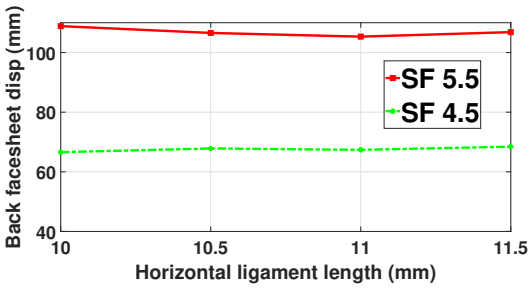
(d) Plastic dissipation

Figure 6: Effect of inclined ligament length (l) on the blast load with a low and high shock factors.

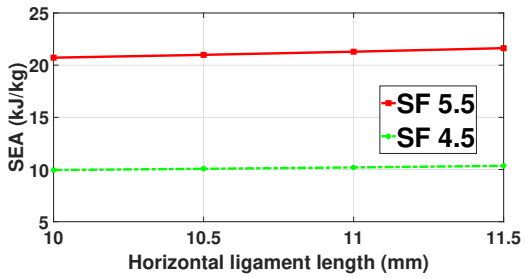
The parametric studies are carried out by increasing one geometric parameter of the re-entrant unit cell at a time, while keeping the remaining parameters fixed at their baseline values. The variation of these geometric parameters ensures that the re-entrant ligaments do not touch each other in the undeformed configuration. However, under blast loading, the ligaments undergo deformation and come into contact with each other due to the incoming load from blast. The effect of the inclined ligament length l on the response of the sandwich plate is shown in Fig. 6 for both $SF = 4.5$ and $SF = 5.5$. For the front facesheet displacement, a decreasing trend with l is observed for both $SF = 4.5$ and $SF = 5.5$, with the rate of decrease being higher for $SF = 5.5$. In the case of the back facesheet, the displacement also decreases with l for both shock factors; however, the decrease is more pronounced compared to the front facesheet, and the variation with l is steeper for $SF = 5.5$ than for $SF = 4.5$. For the specific energy absorption (SEA), a decreasing trend with l is observed for both $SF = 4.5$ and $SF = 5.5$, with the decrease being more pronounced for $SF = 5.5$. In the case of plastic dissipation, the values remain nearly constant with variation in l for both shock factors, indicating that the change in l does not significantly influence the plastic energy dissipation. Overall, the increase in l leads to a reduction in both deformation and energy absorption, while the plastic dissipation remains nearly unaffected.



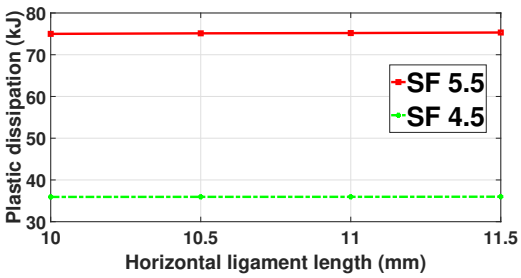
(a) Front facesheet displacement



(b) Back facesheet displacement



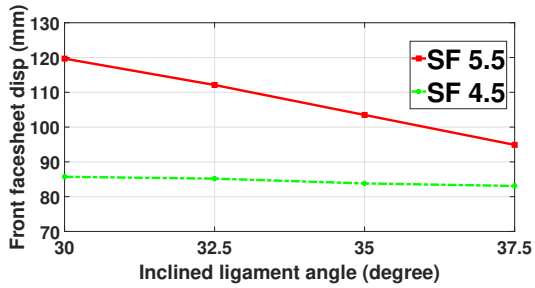
(c) Specific energy absorption



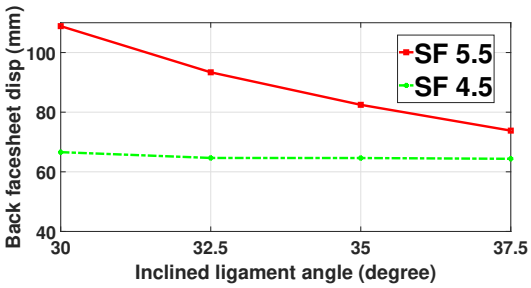
(d) Plastic dissipation

Figure 7: Effect of horizontal ligament length (d) on the blast load with a low and high shock factors.

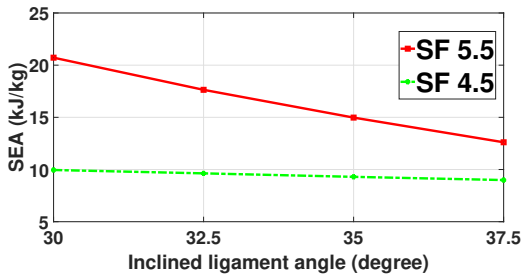
The effect of the horizontal ligament length d on the response of the sandwich plate is shown in Fig. 7. For the front facesheet displacement, the values remain nearly constant with variation in d for $SF = 4.5$, whereas a slight increasing trend is observed for $SF = 5.5$. In the case of the back facesheet, only a very small variation with d is observed for both shock factors. For $SF = 4.5$, the displacement shows a slight increase initially, followed by a marginal decrease and then a small increase again. For $SF = 5.5$, the displacement decreases slightly with increase in d in the initial range and then shows a small increase at the higher value of d. For the SEA, a gradual increase with d is observed for both shock factors, with the change being slightly more noticeable for $SF = 5.5$. In the case of plastic dissipation, the values remain nearly constant with variation in d for both shock factors, indicating that the change in d has very little influence on the plastic energy dissipation. Overall, the variation in d has only a minor influence on the deformation response and SEA, while the plastic dissipation remains nearly unchanged.



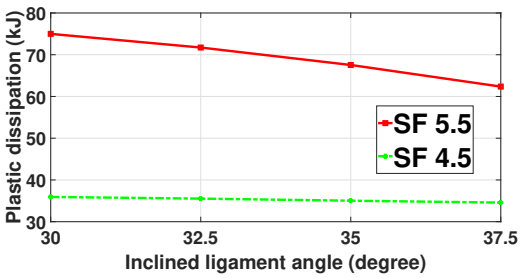
(a) Front facesheet displacement



(b) Back facesheet displacement



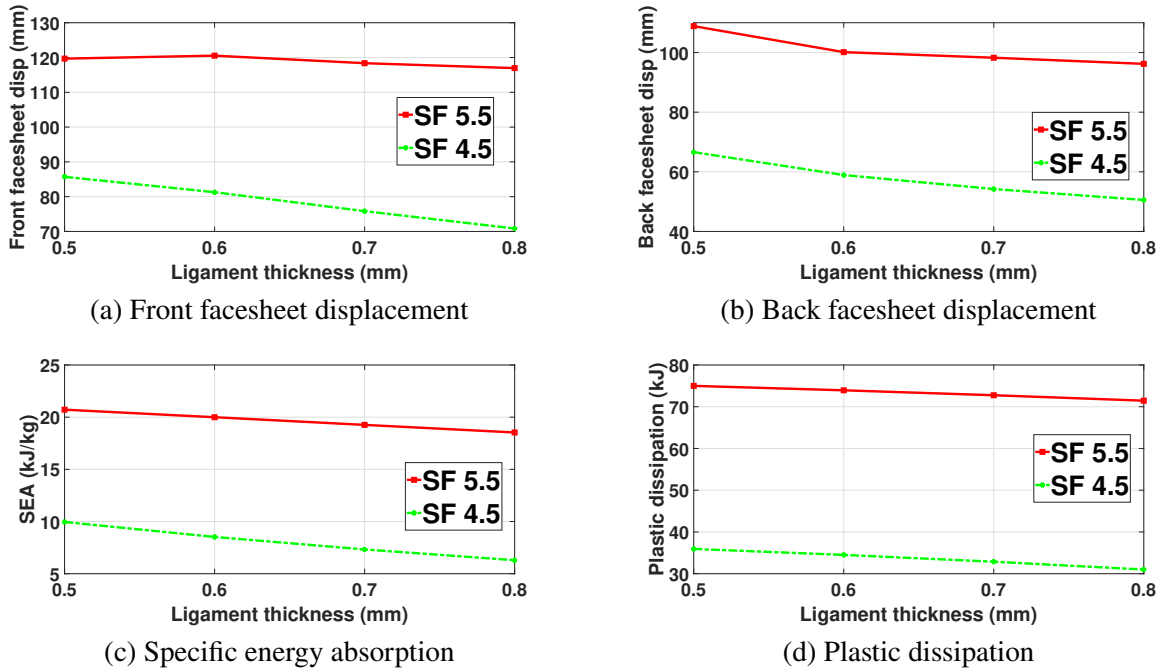
(c) Specific energy absorption



(d) Plastic dissipation

Figure 8: Effect of inclined ligament angle (θ) on the blast load with a low and high shock factors.

The effect of the inclined ligament angle θ on the response of the sandwich plate is shown in Fig. 8 for both $SF = 4.5$ and $SF = 5.5$. For $SF = 4.5$, both the front and back facesheet displacements show a slight decreasing trend with increase in θ. For $SF = 5.5$, a decreasing trend is observed, where both the front and back facesheet displacements reduce with increase in θ, and the reduction in the back facesheet displacement is more pronounced than that of the front facesheet. For the SEA, a decreasing trend with θ is observed for both $SF = 4.5$ and $SF = 5.5$, with the decrease being more pronounced for $SF = 5.5$. In the case of plastic dissipation, the values also decrease with increase in θ for both shock factors, with a slightly higher reduction observed for $SF = 5.5$. Overall, the increase in θ leads to a reduction in both deformation and energy absorption, along with a decrease in plastic dissipation, with the effect being more pronounced under the higher shock factor.



(a) Front facesheet displacement

(b) Back facesheet displacement

(c) Specific energy absorption

(d) Plastic dissipation

Figure 9: Effect of ligament thickness (t) on the blast load with a low and high shock factors.

The response of the sandwich plate with varying ligament thickness t is shown in Fig. 9 for both shock factors. For $SF = 4.5$, both the front and back facesheet displacements decrease with increase in t, and the rate of decrease is nearly the same in both cases. For $SF = 5.5$, the front facesheet displacement shows only a very small variation with t, whereas the back facesheet displacement decreases more noticeably with increase in t. For the SEA, a decreasing trend with t is observed for both $SF = 4.5$ and $SF = 5.5$. The rate of decrease is nearly the same for both shock factors. In the case of plastic dissipation, a slight decrease with increase in t is observed for both shock factors. Overall, the increase in t leads to a reduction in deformation and energy absorption, along with a smaller decrease in plastic dissipation.

5 CONCLUSIONS

The blast response of a sandwich plate with a re-entrant core is investigated through finite element simulations in ABAQUS by considering different geometric parameters and blast load intensities, with the structure modelled using the Johnson–Cook material and damage model. To ensure the reliability of the simulations, the blast loading is first validated, following which the analyses are carried out on the sandwich plate with a re-entrant core.

The key observations from the current work are as follows:

- The increased severity of damage is reflected in the finite element simulations by a greater number of elements undergoing damage as the shock factor increases.
- The front facesheet displacement for higher shock factor decreases with increase in inclined ligament angle (θ) and inclined ligament length (l), and remains nearly unchanged with variation in other geometric parameters. For lower shock factor, the displacement remains almost constant for all geometric parameters except ligament thickness (t), where it decreases with increase in this thickness.

- The back facesheet displacement decreases with increase in geometric parameters for both shock factors, except for horizontal ligament length (d), where the variation is negligible.
- The specific energy absorption (SEA) remains almost unaffected with variation in d for both shock factors, whereas for other geometric parameters, a decreasing trend is observed for both shock factors.
- The plastic dissipation remains nearly constant for the lower shock factor irrespective of changes in geometric parameters. For the higher shock factor as well, it is largely unaffected, with only a slight decrease observed with increase in θ.
- Overall, with increase in geometric parameters, both deformation and SEA decrease for low and high shock factors; however, variation in d does not significantly influence these responses.

The future scope of work will be to conduct optimization studies to determine the geometrical parameters with the objective of minimizing face-sheet displacements, maximizing energy absorption and dissipation, and reducing damage due to blast loads. In addition, experimental studies will be conducted to validate the numerical findings obtained in the present study.

Acknowledgements

The authors express gratitude to the Science and Engineering Research Board, Government of India, for financial assistance (Grant No.: CRG/2023/005148) for this research.

REFERENCES

[1] Kenneth E Evans and KL Alderson. "Auxetic materials: the positive side of being negative". In: *Engineering Science and Education Journal* 9.4 (2000), pp. 148–154.

[2] Xin Ren et al. "Auxetic metamaterials and structures: a review". In: *Smart materials and structures* 27.2 (2018), p. 023001.

[3] Milad Najafi, Hamed Ahmadi, and Gholamhossein Liaghat. "Experimental investigation on energy absorption of auxetic structures". In: *Materials today: proceedings* 34 (2021), pp. 350–355.

[4] M Shokri Rad et al. "Determination of energy absorption in different cellular auxetic structures". In: *Mechanics & Industry* 20.3 (2019), p. 302.

[5] JX Qiao and CQ Chen. "Impact resistance of uniform and functionally graded auxetic double arrowhead honeycombs". In: *International Journal of Impact Engineering* 83 (2015), pp. 47–58.

[6] Chong Li et al. "Low-velocity impact response of sandwich plates with GRC face sheets and FG auxetic 3D lattice cores". In: *Engineering Analysis with Boundary Elements* 132 (2021), pp. 335–344.

[7] Rajendra Prasad Bohara et al. "Anti-blast and-impact performances of auxetic structures: A review of structures, materials, methods, and fabrications". In: *Engineering structures* 276 (2023), p. 115377.

[8] Chang Qi et al. "Impact and close-in blast response of auxetic honeycomb-cored sandwich panels: experimental tests and numerical simulations". In: *Composite structures* 180 (2017), pp. 161–178.

[9] Duc Dinh Nguyen and Cong Hong Pham. “Nonlinear dynamic response and vibration of sandwich composite plates with negative Poisson’s ratio in auxetic honeycombs”. In: *Journal of Sandwich Structures & Materials* 20.6 (2018), pp. 692–717.

[10] Bibhu Prasad Mahapatra et al. “Active vibration suppression of tetrachiral auxetic core sandwich panel with CFRP skin: An RVE homogenization-assisted finite element approach”. In: *European Journal of Mechanics-A/Solids* 106 (2024), p. 105282.

[11] Tiantian Li, Fan Liu, and Lifeng Wang. “Enhancing indentation and impact resistance in auxetic composite materials”. In: *Composites Part B: Engineering* 198 (2020), p. 108229.

[12] LL Hu, M Zh Zhou, and H Deng. “Dynamic indentation of auxetic and non-auxetic honeycombs under large deformation”. In: *Composite Structures* 207 (2019), pp. 323–330.

[13] JackR Vinson. *The behavior of sandwich structures of isotropic and composite materials*. Routledge, 2018.

[14] Solomon Abebe Derseh, Tesfaye Alemu Mohammed, and Girum Urgessa. “Numerical study on hybrid metallic sandwich structures subjected to air burst”. In: *SN Applied Sciences* 5.9 (2023), p. 248.

[15] Nejc Novak et al. “Blast response study of the sandwich composite panels with 3D chiral auxetic core”. In: *Composite Structures* 210 (2019), pp. 167–178.

[16] Chuanqing Chen et al. “Dynamic behaviors of sandwich panels with 3D-printed gradient auxetic cores subjected to blast load”. In: *International Journal of Impact Engineering* 188 (2024), p. 104943.

[17] Alex Remennikov et al. “Development and performance evaluation of large-scale auxetic protective systems for localised impulsive loads”. In: *International Journal of Protective Structures* 10.3 (2019), pp. 390–417.

[18] Dulara Kalubadanage. “Development of negative Poisson’s ratio composite panel system for blast and impact protection”. PhD thesis. University of Wollongong.

[19] Kadir Günaydın and Orhan Gülcan. “Air blast response of sandwich structures with auxetic cores under in-plane and axial loadings”. In: *Res. Eng. Struct. Mater* 9 (2023), pp. 617–630.

[20] Gabriele Imbalzano et al. “Blast resistance of auxetic and honeycomb sandwich panels: Comparisons and parametric designs”. In: *Composite Structures* 183 (2018), pp. 242–261.

[21] Mayank Rai, Anoop Chawla, and Sudipto Mukherjee. “Parametric study of re-entrant honeycomb cored auxetic sandwich panel exposed to blast loading”. In: *Materials Today: Proceedings* 87 (2023), pp. 197–203.

[22] Xiaochao Jin et al. “Dynamic response of sandwich structures with graded auxetic honeycomb cores under blast loading”. In: *Composites Part B: Engineering* 106 (2016), pp. 206–217.

[23] Marcel Walkowiak, Ulf Reinicke, and Denis Anders. “Numerical investigation of different core topologies in sandwich-structured composites subjected to air-blast impact”. In: *Applied Sciences* 12.18 (2022), p. 9012.

[24] Richard Critchley et al. “Blast mitigation using polymeric 3D printed auxetic re-entrant honeycomb structures: A preliminary study”. In: *International Journal of Protective Structures* 13.3 (2022), pp. 469–486.

[25] Dulara Kalubadanage et al. “Close-in blast resistance of large-scale auxetic re-entrant honeycomb sandwich panels”. In: *Journal of Sandwich Structures & Materials* 23.8 (2021), pp. 4016–4053.

[26] Zhen Zou et al. “Blast resistance of sandwich structures consisting of re-entrant honeycombs reinforced by catenary”. In: *Composite Structures* 359 (2025), p. 118995.

[27] Aswanth V Utham, Gaurav Watts, and Radha Raman Mishra. “Numerical assessment of blast performance of a sandwich structure with novel circular re-entrant star honeycomb auxetic core”. In: *Journal of Sandwich Structures & Materials* (2025), p. 10996362251411359.

[28] Yuanhao Zhao et al. “Blast resistance of re-entrant auxetic cored sandwich panels with tunable stiffness”. In: *Scientific Reports* 15.1 (2025), p. 35967.

[29] Yehan Rajapakse, Vignarajah Muthulingam, and Thanuja Kulathunga. “Numerical study on the blast performance of composite foam-filled re-entrant auxetic honeycomb-cored sandwich panels under air blast loading”. In: *2023 Moratuwa Engineering Research Conference (MERCon)*. IEEE. 2023, pp. 25–30.

[30] Gordon R Johnson. “A constitutive model and data for metals subjected to large strains, high strain rates and high temperatures”. In: *Proceedings of the 7th International Symposium on Ballistics, Am. Def. Prep. Org.(ADPA), Netherlands, 1983*. 1983, pp. 541–547.

[31] Gordon R Johnson and William H Cook. “Fracture characteristics of three metals subjected to various strains, strain rates, temperatures and pressures”. In: *Engineering fracture mechanics* 21.1 (1985), pp. 31–48.